

10. MOLECULAR BIOGEOCHEMISTRY OF CRETACEOUS BLACK SHALES FROM THE DEMERARA RISE: PRELIMINARY SHIPBOARD RESULTS FROM SITES 1257 AND 1258, LEG 207¹

Astrid Forster,² Helen Sturt,³ Philip A. Meyers,⁴ and
the Leg 207 Shipboard Scientific Party⁵

ABSTRACT

Shipboard analysis was carried out on the free biomarker fraction of total lipid extracts of 10 Cretaceous black shale samples from Sites 1257 and 1258. The principal aim of the investigation was to study the primary biological sources and the thermal maturity of the organic matter in the core samples as well as the conditions of its preservation. The samples have total organic carbon contents of 4.5–28 wt%. Molecular analysis of biomarkers focused on *n*-alkane, sterane, and pentacyclic triterpane biomarkers. The organic matter in the black shales is thermally immature and dominantly derived from algal and microbial sources with varying contributions of higher plant material. Sulfur incorporation into organic matter is evident from the abundance of hopanoid thiophenes and isorenieratane thianes. High yields of lycopane relative to *n*-C₃₅ indicate that the preservation of organic matter is excellent, which is consistent with deposition under oxygen-depleted conditions in the background of low sedimentation rates.

¹Forster, A., Sturt, H., Meyers, P.A., and the Leg 207 Shipboard Scientific Party, 2004. Molecular biogeochemistry of Cretaceous black shales from the Demerara Rise: preliminary shipboard results from Sites 1257 and 1258, Leg 207. *In* Erbacher, J., Mosher, D.C., Malone, M.J., et al., *Proc. ODP, Init. Repts.*, 207, 1–22 [Online]. Available from World Wide Web: <http://www-odp.tamu.edu/publications/207_IR/VOLUME/CHAPTERS/IR207_10.PDF>. [Cited YYYY-MM-DD]

²Department of Marine Geobiological and Environmental Chemistry, Royal Netherlands Institute for Sea Research, PO Box 59, 1790 AB Den Burg, Texel, The Netherlands. forster@nioz.nl

³Department of Geology and Geophysics, Woods Hole Oceanographic Institution, Mail #22, Woods Hole MA 02543, USA.

⁴Department of Geological Sciences, University of Michigan, 2534 C.C. Little Building, Ann Arbor MI 48109-1063, USA.

⁵Shipboard Scientific Party addresses.

INTRODUCTION

Organic carbon-rich black shales are found extensively in widely different Cretaceous marine settings. Although globally distributed, the black shales are restricted to specific intervals during the Aptian–Santonian ages (see review in Arthur et al., 1990). The mid-Cretaceous is characterized by a coincidence of intensified volcanism, increased oceanic crust production, elevated sea level, and high paleotemperatures that peaked in the early Turonian (Larson, 1991a, 1991b). The concept of global oceanic anoxic events (OAEs) (Schlanger and Jenkyns, 1976) was proposed to explain times of enhanced organic carbon burial associated with the genesis of widespread marine black shales as at the Cenomanian/Turonian (C/T) boundary (OAE 2). The OAEs reflect periods of biotic crisis, likely linked to a limited oxygen supply in already oxygen-depleted warm oceans and epeiric seas. The oxygen restriction in these marine settings could have been reinforced either by an increase in primary organic matter production related to transgressions (Schlanger and Jenkyns, 1976; Jenkyns, 1980), by the onset of density stratification following a decrease in oceanic circulation (e.g., Ryan and Cita, 1977; Fischer and Arthur, 1977), or by a combination of both (Arthur and Schlanger, 1979; Stein, 1986).

During Leg 207, 56- to 93-m-thick intervals of lower Albian–Santonian organic matter-rich black shales were recovered from five different sites. All these sites are located on the northwestern slope of the Demerara Rise, a northwest-southeast-oriented prominent submarine plateau, ~380 km long, offshore Suriname and French Guyana (see the “[Leg 207 Summary](#)” chapter for more comprehensive information). The rock samples included in this study were taken from cores at Sites 1257 and 1258, representing, respectively, the second deepest (2951 meters below sea level [mbsl]) and the deepest (3192 mbsl) locations with regard to water depth.

Site 1257 was drilled to a total depth of 285 meters below seafloor (mbsf) on a terrace above the steep northern flank of the Demerara Rise at the same location as Deep Sea Drilling Project (DSDP) Site 144. A 57-m-thick interval of Cenomanian–Santonian black shales was recovered. These laminated sediments (lithostratigraphic Unit IV) have high total organic carbon (TOC) concentrations (up to 15.8 wt%; average = 6.6 wt%) and were deposited at an estimated sedimentation rate of 0.5 cm/k.y. (see “[Lithostratigraphy](#),” p. 4, “[Organic Geochemistry](#),” p. 22, and “[Sedimentation Rates](#),” p. 21, all in the “Site 1257” chapter).

Site 1258 was drilled ~43 km west of Site 1257 on the gently dipping northwestern slope of the Demerara Rise to a total depth of 485 mbsf. The 56-m-thick black shale interval at Site 1258 (Unit IV) consists of an expanded Cenomanian section overlain by Turonian sediments that are truncated by an erosional unconformity. The sediments of Unit IV have average TOC = 7.9 wt%, but vary between 0.1 and 28.3 wt% (estimated sedimentation rate = 0.3 cm/k.y.) (see “[Lithostratigraphy](#),” p. 4, “[Organic Geochemistry](#),” p. 24, and “[Sedimentation Rates](#),” p. 23, all in the “Site 1258” chapter). The lower to mid-Albian sediments (Unit V) at Site 1258 contain up to 5 wt% TOC and represent an atypical clay-rich facies different from all other sites, where Albian deposits are normally characterized by organic matter-lean siliciclastics (see “[Leg 207 Summary](#)” chapter).

The aim of our investigation focused on establishing biomarker-based evidence for the biological sources and the maturity of the or-

ganic matter and indicators of its depositional environment, especially preservation.

ANALYTICAL METHODS

Ten shipboard samples (four from Site 1257 and six from Site 1258) were chosen for detailed investigation of their biomarker compositions, partly to cover the stratigraphic range of the black shales but primarily on the basis of their TOC contents and the results of Rock-Eval analysis. Because the extractions were performed on samples used for shipboard carbonate analysis, the size of the rock samples was limited.

For the series of extractions on samples from Site 1257, only 1 g of rock powder was used, which sometimes yielded sample concentrations that were too low for optimal gas chromatography-mass selective detector (GC-MSD) analysis (see “[Gas Chromatography-Mass Selective Detector Analysis](#),” p. 4). More material was extracted for the batch of samples from Site 1258, giving better results on the GC-MSD but creating apparent differences in sample quality that affect comparison of results from the two sites. Quantification of compounds could not be done because suitable internal standards were not available on the ship. Thus, samples are evaluated in qualitative terms by employing biomarker ratios.

Extraction

All samples were extracted ultrasonically; freeze-dried, powdered sediment (1–6 g) was placed in a 100-mL centrifuge tube with ~8 mL of dichloromethane (DCM). The samples were sonicated for 30 min and allowed to settle. The clear supernatant layer was transferred into a clean vial. The residue was extracted a second time, and both extracts were combined. The extract was filtered through a small Pasteur pipette plugged with precleaned cotton wool into a clean preweighed vial. A small piece of clean aluminum foil was placed under the screw lid to prevent sample contamination. The solvent was evaporated under nitrogen, and the weight of the total lipid extract was measured.

Elemental Sulfur Removal with Activated Copper

The total lipid extracts were treated with acid-activated copper to remove elemental sulfur, which could interfere with GC-MSD analysis. Copper wire normally employed in the Rock-Eval instrument was placed in an Erlenmeyer flask, and a small amount of concentrated (37%) hydrochloric acid was added. When the copper reached its bright typical color, the acid was decanted and the copper was rinsed with nanopure water until pH neutral, then with methanol (seven times), and finally with DCM (seven times).

Small amounts of activated and cleaned copper were added to the vials containing the extracts in DCM, and the samples were magnetically stirred overnight (~8 hr). Blackening of the copper indicated reaction with elemental sulfur present in the sample. Each extract dissolved in DCM was then filtered over a cotton wool-plugged Pasteur pipette to remove the copper and was subsequently evaporated to dryness under nitrogen.

Extract Fractionation

Silica gel (Fisher 100–200 mesh) was activated by heating at 120°C overnight, cooled in a dessicator, and made into a slurry with hexane. Pasteur pipettes were plugged with cotton wool and filled with the slurry. Extracts were dissolved in hexane and added to the top of the column. Fractions of increasing polarity were collected by sequential elution with 4 mL each of hexane (aliphatic fraction), DCM/hexane (1:1) (aromatic fraction), and DCM (polar fraction). The eluates were collected in clean preweighed vials, the solvent was removed under nitrogen, and the mass of each extract was recorded as precisely as possible under shipboard conditions. No internal standard was added.

Gas Chromatography-Mass Selective Detector Analysis

The aliphatic, aromatic, and polar fractions were dissolved in hexane and transferred to autosampler vials for analysis on the GC-MSD, a Hewlett-Packard (HP) system consisting of an HP 6890 GC with an HP 5973 MSD and an HP 7683 automatic liquid sampler (ALS). The GC was equipped with an electronic program controlled (EPC) split-splitless injector and an HP capillary column (5% phenyl methyl siloxane; 30 m × 0.25 μm) programmed from 70° to 130°C at 20°C/min, then at 4°C/min to 320°C, and held at 320°C for 20 min. Helium was used as the carrier gas. The transfer line was set at 280°C, and the MSD source was set at 230°C. A heated interface connects the capillary column from the GC to the mass spectrometer, where electron impact (EI)-mass spectra were acquired at 70 eV in full scan mode (scan range from $m/z = 27$ –800). An electron multiplier system served as detector. Data were acquired and processed by HP MS-ChemStation software. Compounds were identified by their relative retention times and by comparison with mass spectra reported in the literature.

RESULTS

Sample Characteristics

Table T1 summarizes the stratigraphic and bulk rock characteristics of the 10 samples included in this investigation. Samples were chosen in an attempt to represent all different-age black shale units; unfortunately, no Santonian samples suitable for extraction were available. The samples vary in their CaCO₃ contents, reflecting the typical layer-by-layer scale lithologic changes caused by the alternation of calcite-rich laminae and clay-dominated black shale intervals. The TOC contents range from 4.5 to 28 wt% and are >8 wt% for all but one sample. Thus, the selection of samples is skewed toward the TOC-rich black shale facies (cf., Tables T16, p. 101, in the “Site 1257” chapter and T16, p. 106, in the “Site 1258” chapter). This bias is also evident from the Rock-Eval parameters, where the hydrogen index (HI) values are all >480 mg HC/g coupled with low (<70 mg CO₂/g) oxygen index (OI) values (Table T1) (cf. Tables T17, p. 104, in the “Site 1257” chapter and T17, p. 111, in the “Site 1258” chapter). The Rock-Eval results (see van Krevelen-type diagrams in Figs. F15, p. 56, in the “Site 1257” chapter and F19, p. 66, in the “Site 1258” chapter) indicate a Type II kerogen typical of algal and microbial primary production (Espitalié et al., 1977; Peters, 1986; Baskin, 1997). For most of the samples, the T_{max} value is below or close

T1. Organic matter properties, p. 19.

to 400°C, indicating a low thermal maturity for the organic matter. The exception is Sample 207-1258C-31R-2, 26–27 cm, of Albian age, which has a slightly higher T_{max} of 415°C but still falls within the immature range.

A positive correlation between the TOC and extract yields ($r^2 = 0.88$) is evident, although errors in weighing under the shipboard conditions limit confidence in this specific correspondence. The extracts differ in color (Table T1). Bright red and orange colors may indicate the presence of porphyrins and other derivatives of biopigments. Three samples showed weak to strong fluorescence under ultraviolet light, and in extract of Sample 207-1258C-31R-2, 26–27 cm, fluorescence was visible even under normal laboratory lighting.

BIOMARKERS

Aliphatic Fractions

Biomarker analysis of aliphatic fractions focused on three groups of compounds, *n*-alkanes, steranes and sterenes, and pentacyclic triterpanes and their derivatives. The results based on integration of peaks in various ion chromatograms are summarized in Tables T2 and T3. Table T2 presents biomarker parameters that describe the thermal maturity and conditions of organic matter preservation based on selected biomarker ratios. Table T3 focuses on biomarkers ratios indicative of their biological sources and their relative distributions in the samples.

Acyclic Alkanes and Isoprenoid Hydrocarbons

n-Alkanes and isoprenoid hydrocarbons were identified from their mass spectra in the total ion chromatogram (TIC) and the m/z 57 ion chromatogram, which was also used for peak integration (Fig. F1A, F1B). *n*-Alkanes range from *n*-C₁₃ to *n*-C₃₅, homologs less than C₁₆ are not observed in most samples, probably because of the loss of these more volatile compounds during sample processing. Isoprenoids were typically identified from their elevated m/z 183 fragment in the mass spectra and their molecular ion (M^+). Pristane (C₁₉H₄₀; M^+ = 268), phytane (C₂₀H₄₂; M^+ = 282), and lycopane (C₄₀H₈₂; M^+ = 562) were present in all samples, and farnesane (C₁₅H₃₂; M^+ = 212) was found in some samples.

Lycopane coelutes with *n*-C₃₅ but can be identified from elevated m/z 113, 253, and 183 fragments (Kimble et al., 1974). The contribution of lycopane to the peak in the m/z 57 ion trace can be inferred from the prominence of the three diagnostic fragments above, ions attributed to *n*-alkyl fragments (fig. 1 in Sinninghe Damsté et al., 2003). On this basis, the coeluting peaks of lycopane and *n*-C₃₅ in all samples consist almost exclusively of lycopane. Lycopane was found in high abundance in all samples; in three it was the most abundant compound (MAC) in the m/z 57 trace (Table T3).

The most abundant compound in the aquatic range of *n*-alkanes between C₁₆ and C₁₈ is presented in Table T3 (C_{max} aquatic). The sources of these *n*-alkane homologs are typically aquatic algae or cyanobacteria (e.g., Blumer et al., 1971; Gelpi et al., 1970; Han and Calvin, 1969; review in Brassell et al., 1978), although the samples differ with respect to their most abundant compound. Phytane predominates in two cases

T2. Organic matter thermal maturity, p. 20.

T3. Biomarker source indicators, p. 21.

F1. *n*-Alkanes and isoprenoids, p. 17.

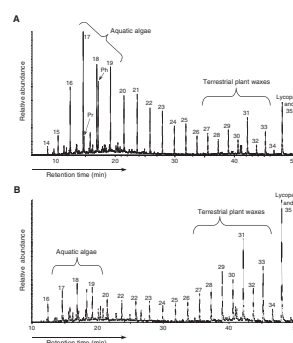


(Table T3). *n*-Alkanes with 23–33 carbon atoms, and especially these from *n*-C₂₇ to *n*-C₃₃, originate from waxes typical of higher land plants. Exclusively for immature organic matter, the predominance of odd- vs. even-numbered *n*-alkanes can be employed as a measure of the proportion of terrestrially derived components. The carbon preference index (CPI) (Bray and Evans, 1961) is a mathematical expression of the odd over even predominance between *n*-C₂₄ and *n*-C₃₄. According to Table T3, the samples show greater uniformity in terms of their dominant compound in the plant wax-derived *n*-alkane range (C_{max} waxes); for most samples this is *n*-C₃₁.

Regular Steranes and Sterenes

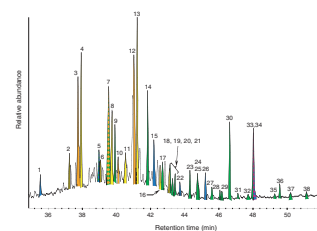
Steranes and sterenes are derived from the sterols of cell membranes of eukaryotes, mainly algae and higher plants (overview in Mackenzie et al., 1982). A wide variety of their stereoisomers is present. The occurrence of unsaturated (sterenes) or rearranged compounds (diasterenes; *m/z* 257) is largely a function of the thermal maturity of the organic matter. The 5 α ,14 α ,17 α (H)-20R (5 $\alpha\alpha\alpha$ -R) isomers of three regular steranes, cholestane (C₂₇; M⁺ = 372), 24-methylcholestane (C₂₈; M⁺ = 386), and 24-ethylcholestane (C₂₉; M⁺ = 400) are clearly the dominating compounds in the *m/z* 217 ion chromatogram and in the TIC (see peaks 4, 8, and 13 in Fig. F2; Table T4). Their relative abundances are given in Table T3 as a percentage, which shows that C₂₇ and C₂₉ steranes are always more abundant than those of C₂₈. No 14 β ,17 β (H)- or 20S-isomers were found, but minor amounts of C₂₇–C₂₉ steranes with 5 β ,14 α ,17 α (H)-20R configuration were detected (peaks labeled 2, 6, and 11 in Fig. F2; Table T4).

Based on the ion chromatogram for *m/z* 257, nine unsaturated steroid hydrocarbons were recognized. Three ster-4-enes (elevated fragment *m/z* 108) represent a large portion of this specific biomarker group in the TIC trace (peaks 3, 7, and 12 in Fig. F2; Table T4). Ster-5-enes, which coelute with 5 α ,14 α ,17 α (H)-20R-steranes (Table T4), can be recognized in the *m/z* 257 ion trace, where they elute as relatively smaller peaks directly after the ster-4-enes. Compounds whose identities could not be assigned are a pair of C₂₉-steradienes (M⁺ = 396) (peak 10 in Fig. F2; Table T4) and a methyl-C₃₀-sterane coeluting with a methyl-C₃₀-sterene (peak 16 in Fig. F2; Table T4).

Hopanes and Rearranged Hopanes/Hopenes

Hopanes found in the aliphatic fraction are pentacyclic triterpenoids derived from cell membranes of prokaryotes (heterotrophic bacteria and also phototrophic cyanobacteria) (e.g., Ourisson et al., 1987; Ourisson and Rohmer, 1992). This biomarker group is, like the steranes, characterized by numerous maturity-sensitive stereoisomers (Seifert and Moldowan, 1980). It was possible to identify the majority of compounds in the *m/z* 191 trace. C₃₀ to C₃₅ 17 α ,21 β (H)- and 17 β ,21 α (H)-hopanes are prominent compounds with 22R-isomers dominating 22S-isomers but subordinate to 17 β ,21 β (H)-hopanoids. Most samples contain many unsaturated or rearranged compounds, including 30-norhop-17(21)-ene, 30-norneo-13(18)-ene, and hop-17(21)-ene. Various norhopanes are also present in all samples, including 17 α - and β -trisnorhopane (C₂₇), 17 α ,21 β (H)-30-norhopane and 17 β (H)21 α (H)-30-norhopane, and 17 β ,21 β (H)-30-norhopane.

F2. Biomarker TIC, p. 18.



T4. TIC biomarkers, p. 22.

Two late-eluting peaks (at 56.6 and 60.6 min; not shown in Fig. F2) are present in nearly all samples. They were identified as 30-(2'-methylenethienyl)-17 α ,21 β (H)- and -17 β ,21 β (H)-hopane (hopanoid thiophenes: M^+ = 508; elevated m/z 97 fragment for both; elevated m/z 287 fragment for the latter compound) (Valisolalao et al., 1984). 2-Methylhopanoids (m/z 367, 383, and 205), which are indicative of contributions from cyanobacteria (e.g., Summons et al., 1999), were not detected.

Aromatic Fraction

The aromatic fractions were searched specifically for isorenieratane and related isorenieratene derivatives (m/z 133). Isorenieratene is a carotenoid pigment exclusively synthesized by photoautotrophic green sulfur bacteria (Chlorobiaceae) and therefore is indicative for euxinic conditions reaching into the photic zone (e.g., Sinninghe Damsté et al., 1993). The molecule isorenieratane itself (M^+ = 546) was identified only in Sample 207-1258B-46R-2, 56–57 cm, coeluting with a hopanoid thiophene at 56.6 min (Table T2). In this sample, a variety of the S-containing isorenieratene derivatives previously described by Koopmans et al. (1996b) are present, together with several isomers of isorenieratane thianes (M^+ = 576) and thiophenes (M^+ = 572) and other isorenieratene derivatives (e.g., diaryl isoprenoids; M^+ = 538). Isorenieratane thianes, but none of the other derivatives of isorenieratene, were abundant in four other samples (Table T2).

Source-specific long-chain alkenones—known to be derived from marine Prymnesiophyta (e.g., Marlowe et al., 1990)—were not found in our investigation. They have been recently reported for even older organic matter-rich sediments from the Aptian OAE 1a obtained during Leg 198 on Shatsky Rise in the Pacific Ocean (Sites 1207 and 1213) (Bralower, Premoli Silva, Malone, et al., 2002). Our preliminary results do not necessarily confirm the absence of these compounds at Sites 1257 and 1258 because our investigation was hampered by the low-response detection problem of the shipboard GC-MSD for masses greater than m/z 500. In this respect, reanalysis of the samples on a more sensitive instrument would be advisable.

Fluorescent samples, especially Sample 207-1258C-31R-2, 26–27 cm (Table T1), contain higher amounts of the pentacyclic aromatic hydrocarbon perylene (M^+ = 252) than nonfluorescing samples. This molecule is the single most abundant polycyclic aromatic hydrocarbon found in the black shales sampled in this study.

INTERPRETATION AND APPLICATION

Maturity Evaluation

The fundamental principle of maturity evaluation by biomarker analysis is based on the structural modification of compounds by stepwise transformation from biological precursor molecules to thermodynamically more stable geochemical fossils. Generally, the form of biologic precursor molecules is defined by their function (e.g., as a part of the cell membrane) and not by thermodynamic stability of the structure. Diagenetic pathways lead to sequential structural rearrangements to more stable molecules, lowering enthalpy while increasing entropy. Thermodynamic equilibrium is eventually reached, which defines the

endpoint of the transformation and determines the final ratio of isomers or products.

The biomarker composition of the apolar fractions of all samples is dominated by hopanes and steranes retaining their biological, and therefore thermally immature, structural configurations. Selected maturity parameters based on biomarkers (Table T2) show no major differences between the two sites in terms of overall maturity. A low thermal maturity is indicated by the presence of $5\beta\alpha\alpha$ -R C_{27} to C_{29} steranes along with the more abundant $5\alpha\alpha\alpha$ -R isomers. $20S$ -isomers of the latter compounds were not detected, nor were their $5\alpha\beta\beta$ -configurations. $\beta\beta$ -hopanes dominate over all other homologous series of hopane isomers, and the abundance of $22S$ -isomers is significantly lower than that of $22R$ -isomers for C_{30} and C_{31} (Table T2), consistent with sediment immaturity.

For most samples, a significant suite of different steranes and hopanes is present, indicating low thermal maturity of the organic matter, which agrees with the low T_{\max} values of the Rock-Eval pyrolysis (Table T1). In addition, it suggests little thermal modification of the kerogen, which implies that the n -alkane distribution of the samples likely represents their unaltered, original composition. Measures, such as the CPI, that are affected by maturation can therefore be applied, although low maturity also produces a potential bias in the distributions of free biomarker fractions because they fail to reflect contributions of organic matter still bound into the kerogen or other macromolecular fractions (Koopmans et al., 1996a). The homohopane index may reflect this bias because the abundance of compounds formed from pentakishomohopanes might be expected to be limited until catagenesis (Köster et al., 1997). Similarly, the pristane/phytane ratio may be influenced by maturity because the abundance of both compounds in the free hydrocarbon fraction is strongly affected by thermal generation of these compounds from precursors and liberation from the bound biomarker fraction (Koopmans et al., 1999). Consequently, the pristane/phytane ratio as given in Table T3 should not be used for the assessment of oxygen levels in the paleoenvironment (Volkman and Maxwell, 1986, see below).

Source Evaluation

The fundamental principle in assessing of biological sources of organic matter using biomarkers is utilization of source-specific compounds. Some compounds indicate a general source (e.g., Brassell et al., 1978; Ourisson et al., 1987); others such as certain isoprenoids or carotenoids (e.g., isorenieratene) are highly source specific (e.g., Brassell et al., 1981; Volkman, 1988).

One example of the general source indicators is the short- vs. long-chain n -alkanes derived from aquatic algal/microbial and higher plant sources, respectively. For most samples, the n -alkane distribution is dominated by n - C_{16} to n - C_{18} (Table T3), indicating a dominant marine source for the n -alkanes. An odd over even carbon number predominance (given as CPI in Table T3) is observed starting at n - C_{23} or n - C_{25} , with n - C_{29} to n - C_{31} being the most abundant higher range compound. The ratio of n - C_{17}/n - C_{31} given in Table T3 is a simplified parameter that reflects relative contributions of aquatic/marine and terrestrial n -alkanes. Evidently, the proportion of land-plant material present in the samples varies through time. Samples 207-1258B-44R-4, 75–76 cm, and

51R-2, 40–41 cm, represent the marine end-members (Table T3), and Samples 207-1258C-31R-2, 26–27 cm, and 207-1257B-22R-1, 44–45 cm (Fig. F1B; Table T3), represent the terrestrial end-members of this binary system. Degradation of organic matter can alter the *n*-alkane distribution and thereby modify the source signal by enriching the more stable land-derived fraction through enhanced loss of the more labile aquatic lipids (Sinninghe Damsté et al., 2002). Thus, the predominant marine signature in the *n*-alkane distributions of most samples also suggests overall good preservational conditions.

The isoprenoids pristane and phytane are primarily derived from the phytol sidechain of the chlorophyll molecule (e.g., Didyk et al., 1978; review in Volkman and Maxwell, 1986) and can be used as biomarkers for phytoplankton. However, other primary sources, such as archaeobacterial ether lipids for both molecules (Didyk et al., 1978), or tocopherols for pristane (Brassell et al., 1983a; Goossens et al., 1984), have been proposed (review in Koopmans et al., 1999). These alternate origins could complicate the source pristane-phytane interpretation in the paleoenvironmental setting at the Demerara Rise, especially possible archaeal contributions.

The source for lycopane in the marine environment is not clear, as neither the molecule itself nor potential precursors have been found in the lipids of a specific group of marine organisms yet. Possible sources are prokaryotes (methanogenic archaea) (e.g., Brassell et al., 1981) or, alternatively, photoautotrophic algae (e.g., Wakeham et al., 1993; overview in Sinninghe Damsté et al., 2003). Corroborating evidence for the latter source in aquatic settings stems from the stable carbon isotopic composition of lycopane analyzed in seawater and various recent and ancient marine sediments (Wakeham et al., 1993; Sinninghe Damsté et al., 2003) and the detection of lycopadiene in a specific strain of the green algae *Botryococcus braunii* (Metzger et al., 1990). However, *B. braunii* is a freshwater species, and it remains unclear how lycopane is preferably generated from this unsaturated precursor (Wakeham et al., 1993). According to Sinninghe Damsté et al. (2003), the high abundance of lycopane in the samples investigated here more likely has stronger implications for the state of water-column oxygenation than for the rate of primary production. Comet et al. (1981) reported a lycopane-dominated *n*-alkane distribution with an entirely marine signature from a laminated upper Albian limestone sample (TOC = 2.1 wt%) from the Hess Rise (northwest Pacific, DSDP Leg 62, Site 465). They proposed an oxygen-depleted water-column setting analog to an oxygen-minimum zone overlain by waters characterized by high algal productivity. Examples of European and Tunisian marine Cenomanian/Turonian black shales yielding lycopane are given in Farrimond et al. (1990).

A widely used tool for paleoenvironmental and source assessment of sedimentary organic matter employs the relative abundances of the C₂₇, C₂₈, and C₂₉ (ααα-R steranes) (e.g., Moldowan et al., 1985; Peters and Moldowan, 1993) as proxies for their eukaryotic sterol precursors (e.g., Mackenzie et al., 1982). Originally, this approach was based on the observation that C₂₈ sterols dominate in phytoplankton (green algae and diatoms), C₂₇ sterols are typical for zooplankton and red algae, and C₂₉ sterols occur in higher plants and some strains of brown or green algae (Huang and Meinschein, 1979). However, care has to be taken when utilizing sterane compositions, as these source assignments are simplified (review in Volkman, 1986, 1998). It is, for example, problematic that the biological sources of the C₂₇ and C₂₉ steranes that are the most

dominant compounds in the Demerara Rise setting cannot actually be differentiated. There is little correlation between the abundances of the C₂₉ sterane and *n*-C₃₁ (Table T3), which implies either different terrigenous sources for both compounds or that the C₂₉ sterane cannot be interpreted as a terrestrial marker here. Nevertheless, there are pronounced differences in the distributions of regular steranes at different stratigraphic levels (Table T3), but it remains unknown if these reflect actual changes in the composition of the algal community. As an example, the ratio of C₂₈/C₂₇- $\alpha\alpha\alpha$ -R steranes more or less increases upsection at both sites (Table T3).

Hopanes represent a biomarker group derived exclusively from prokaryotic sources (Ourisson et al., 1979). Generally, they are nonspecific for any group of bacteria or other microbes. To estimate the temporal variation of contributions of eukaryotic vs. prokaryotic sources, the sum of all sterane compounds (*m/z* 217) and all hopanes (*m/z* 191) has been utilized as the sterane/hopane ratio given in Table T3. However, by employing *m/z* 217 for integration of the sterane compounds, this ratio appears to be biased toward enhancing the hopane group for these immature samples. The abundance of steranes/sterenes and hopanes/hopenes in the TIC biomarker spectrum as shown in Figure F2 clearly indicates that both algal and microbial sources more or less equally contribute to biomarker assemblage in high amounts. To compensate for this bias, the ratio needs to be corrected by some factor or the TIC should be used for its calculation. Nevertheless, the large proportion of prokaryotic biomarkers seems quite unusual for a normal marine setting but is well known from other marine Cretaceous black shale deposits. Examples are lower Aptian deposits (OAE 1a; Leg 198, Sites 1207 and 1213, Shatsky Rise, northeast Pacific; Bralower, Premoli Silva, Malone, et al., 2002), Turonian sediments (Leg 75, DSDP Site 530, Angola Basin, southeast Atlantic; Brassell, 1984), and Cenomanian/Turonian sediments in marine settings in Europe and Tunisia (OAE 2; Farrimond et al., 1990).

Something that remains for further investigation is the origin and significance of the high abundance of perylene in some samples (see “**Aromatic Fraction**,” p. 7, in “Biomarkers”). The source for perylene is still not known, but it may represent an early stage diagenetic product formed in sediment from nonspecific precursors (Wakeham et al., 1979; Silliman et al., 2000).

Assessment of Paleoenvironment/ Preservational Conditions

The quality of organic matter preservation can be estimated by the degree of degradation of sensitive geochemical compounds and the presence of labile compounds such as carbohydrates or pigments. As the organic matter at Sites 1257 and 1258 is immature and prokaryotic sources for phytane cannot be ruled out (see “**Maturity Evaluation**,” p. 7, and “**Source Evaluation**,” p. 8), a classical parameter, the pristane/phytane ratio (Didyk et al., 1978) (Table T3), should not be employed as a strict measure for the degree of oxygen depletion in the water column. However, the low values stated in Table T3 are like those reported from other marine Cretaceous black shales of comparably low thermal maturity (e.g., Bralower, Premoli Silva, Malone, et al., 2002; Brassell et al., 1983b; Comet et al., 1981; Didyk et al., 1978; Meyers et al., 1984). This similarity could indeed imply that the paleoenviron-

mental conditions at the Demerara Rise provided a suitably reducing setting in which the generation of phytane from phytol could have taken place. However, even if we assume that thermal maturity does not have a biasing influence on the proportions of pristane and phytane here, additional prokaryotic sources for phytane cannot be ruled out.

The homohopane index (Table T2; note modification of index used here) is the percentage of the pentakis-homohopanes (C_{35}) vs. the total of all homohopanes ($\Sigma C_{31}-C_{35}$). The index is based on the premise that the longer sidechain molecules C_{33} to C_{35} are only preserved under anoxic conditions (Peters and Moldowan, 1991), for example by sulfur incorporation (Köster et al., 1997). In dysoxic to oxic settings, oxidation and subsequent decarboxylation of the original C_{35} -precursor molecules lead to a shortening of the sidechain so that C_{31} - to C_{32} -homohopanes are generated. The samples from Site 1258 show a slightly higher homohopane index on average than those from Site 1257. If the homohopane index is not affected by other factors, this would speak to a somewhat more oxygen-depleted setting at Site 1258.

Hopanoid thiophenes are present in all samples, which suggests that sulfur incorporation into the organic matter has taken place throughout the entire black shale sequence at both sites, most likely at an early diagenetic stage (e.g., Werne et al., 2000). The ratio of hopanoid thiophenes over C_{30} -hopanes is also slightly higher in samples from Site 1258 than in those from Site 1257 (Table T2). This might point toward a higher rate of sulfur incorporation into the organic matter at Site 1258 if influences by other factors (e.g., differences in the abundance of precursor molecules or sedimentation rates) can be ruled out. Incorporation of inorganic sulfur species into organic matter enhances the preservation of labile compounds such as carotenoids or carbohydrates (e.g., Kok et al., 2000) but also implies that a substantial quantity of these reactive compounds is captured in the bound-biomarker fraction of these immature samples. In this case, paleoenvironmental interpretations cannot be based solely on the abundance of isorenieratane or its derivatives in the free-biomarker fraction but need to be corroborated by analysis of the sulfur-bound isorenieratane.

Kuypers et al. (2002) found sulfur-bound isorenieratane in elevated concentrations in sediments from just below the Cenomanian/Turonian boundary at DSDP Site 144, which has been redrilled as Site 1257 during Leg 207. They also reported its occurrence in lower concentrations for sediments below the onset of the isotopic excursion of OAE 2 and concluded that sulfur-containing anoxic water masses must have periodically reached the photic zone before the onset of OAE 2. Our investigation at Sites 1257 and 1258 was limited to the free-biomarker fraction and mainly isorenieratane thianes that were found in five samples (Table T2); hence, further interpretations should be reserved until more comprehensive studies, including the bound-biomarker fraction, are done. Interestingly, isorenieratane and several other isorenieratane derivatives were found in the aromatic fraction of Sample 207-1258B-46R-2, 56–57 cm. This sample is unusually rich in organic matter (TOC = 28 wt%) (Table T2) and, according to biostratigraphy, is situated closely below the Cenomanian/Turonian boundary (see “Biostratigraphy,” p. 10, in the “Site 1258” chapter), which probably places it within the OAE 2 range.

Lycopane offers perhaps the best potential for addressing questions of oxygen paleolevels in the water column, as its concentration in the

free hydrocarbon biomarker fraction is not a function of thermal maturity and it is not known to be prone to diagenetic sulfurization (Sinninghe Damsté et al., 2003). Sinninghe Damsté et al. (2003) propose the ratio of lycopane vs. $n\text{-C}_{31}$ as a measure for the paleoredox conditions during sediment deposition based on data from the oxygen minimum zone (OMZ) of today's Arabian Sea. They reported an increase of the $(\text{lycopane} + n\text{-C}_{35})/n\text{-C}_{31}$ ratio from values of ~ 0.3 for sediments above and below the OMZ to unity or even higher within the OMZ. The ratios for $(\text{lycopane} + n\text{-C}_{35})/n\text{-C}_{31}$ given in Table T2 are >1 for all but the Albian sample. However, the amount of terrestrially derived long-chain n -alkanes (namely $n\text{-C}_{31}$) varies significantly in these samples, which affects the ratio, yet the high abundance of lycopane implies that black shale sedimentation took place under strongly oxygen depleted conditions. Better constraints on the sedimentation rates estimated for the black shale interval (0.5 cm/k.y. for Site 1257 and 0.3 cm/k.y. for Site 1258) (see "Sedimentation Rates," p. 21, in the "Site 1257" chapter and "Sedimentation Rates," p. 23, in the "Site 1258" chapter) would help improve these paleoenvironmental interpretations.

IMPLICATIONS FOR BLACK SHALE GENESIS ON THE DEMERARA RISE

Identification of isorenieratane and isorenieratane derivatives from Leg 207 samples is consistent with previous work (Kuypers et al., 2002) that shows intermittent events of photic zone anoxia must have taken place during the deposition of the Cretaceous black shales at the Demerara Rise, even though the timing and extent of these events cannot be resolved. The repeated recurrence of organic matter-rich black shales suggests that excellent conditions for organic matter preservation occurred during Albian–Santonian time.

The low sedimentation rates appear to contradict high-productivity conditions as a major driving factor for anoxia, which would be needed to explain the genesis of black shales on the Demerara Rise. However, sedimentation could have been affected by postdepositional reworking of material (erosion or winnowing processes) on the seafloor or, at least partially, by dissolution of the carbonate phase in the sediments, both leading in consequence to lowered sedimentation rates. An alternative way of maintaining oxygen-depleted conditions in the water column over such a long timespan is to assume permanent stratification (e.g., of the silled basin type) or to import anoxia from a more distal and deeper location in the proto-Atlantic Ocean (stagnating ocean model for Cretaceous black shales) by upwelling of strongly O_2 -depleted oceanic water masses. This latter interpretation is consistent with the idea of stagnant Cretaceous oceans and would explain how large amounts of sulfur could be provided for its incorporation into the organic matter. However, higher sedimentation rates would favor the buildup of an expanded and permanent OMZ mainly driven by elevated surface water bioproductivity as a likely alternative scenario for the Cretaceous black shale sedimentation on the Demerara Rise.

SUMMARY

Organic matter in the 10 Cretaceous black shale samples from Sites 1257 and 1258 is thermally immature, as indicated by sterane and hopane biomarkers that remain in their most immature structural configurations. Distributions of *n*-alkanes, steranes, and hopanes extracted from the black shales indicate that they are derived from a mostly algal and microbial source with varying contributions of land-plant material. Good preservation of organic matter implies a strongly oxygen depleted depositional setting, especially considering the generally low sedimentation rates.

ACKNOWLEDGMENTS

We thank Lisa Brandt, Dennis Graham, and Chieh Peng for their assistance in the laboratory and with the GC-MSD. Jaap Sinninghe Damsté provided crucial information for identification of lycopane and the hopanoid thiophenes. The manuscript benefited from a thoughtful review by Simon Brassell.

REFERENCES

- Arthur, M.A., Jenkyns, H.C., Brumsack, H.J., and Schlanger, S.O., 1990. Stratigraphy, geochemistry, and paleoceanography of organic carbon-rich Cretaceous sequences. In Ginsburg, R.N., and Beaudoin, B. (Eds.), *Cretaceous Resources, Events and Rhythms: Background and Plans for Research*. NATO ASI Ser., Ser. C, 304:75–119.
- Arthur, M.A., and Schlanger, S.O., 1979. Cretaceous “oceanic anoxic events” as causal factors in development of reef-reservoired giant oil fields. *AAPG Bull.*, 63:870–885.
- Baskin, D.K., 1997. Atomic H/C ratio of kerogen as an estimate of thermal maturity and organic matter conversion. *AAPG Bull.*, 81:1437–1450.
- Blumer, M., Guillard, R.R.L., and Chase, T., 1971. Hydrocarbons of marine phytoplankton. *Mar. Biol.*, 8:183–189.
- Bralower, T.J., Premoli Silva, I., Malone, M.J., et al., 2002. *Proc. ODP, Init. Repts.*, 198 [Online]. Available from World Wide Web: <http://www-odp.tamu.edu/publications/198_IR/198ir.htm>. [Cited 2003-03-24]
- Brassell, S.C., 1984. Aliphatic hydrocarbons of a Cretaceous black shale and its adjacent green claystone from the southern Angola Basin, Deep Sea Drilling Project, Leg 75. In Hay, W.W., Sibuet, J.C., et al., *Init. Repts. DSDP, 75* (Pt. 2): Washington (U.S. Govt. Printing Office), 1019–1030.
- Brassell, S.C., Eglinton, G., and Maxwell, J.R., 1983. The geochemistry of terpenoids and steroids. *Biochem. Soc. Trans.*, 11:575–586.
- Brassell, S.C., Eglinton, G., Maxwell, J.R., and Philp, R.P., 1978. Natural background of alkanes in the aquatic environment. In Hutzinger, O., van Lelyveld, L.H., and Zoeteman, B.C.J. (Eds.), *Aquatic Pollutants: Transformation and Biological Effects*: Oxford (Pergamon Press), 69–86.
- Brassell, S.C., Howell, V.J., Gowar, A.P., and Eglinton, G., 1983. Lipid geochemistry of Cretaceous sediments recovered by the Deep Sea Drilling Project. *Adv. Org. Geochem. Proc. Int. Meet.*, 10th, 477–484.
- Brassell, S.C., Wardroper, A.M.K., Thomson, I.D., Maxwell, J.R., and Eglinton, G., 1981. Specific acyclic isoprenoids as biological markers of methanogenic bacteria in marine sediments. *Nature*, 290:693–696.
- Bray, E.E., and Evans, E.D., 1961. Distribution of *n*-paraffins as a clue to recognition of source beds. *Geochim. Cosmochim. Acta*, 22:2–15.
- Comet, P.A., McEvoy, J., Brassell, S.C., Eglinton, G., Maxwell, J.R., and Thomson, I.D., 1981. Lipids of an upper Albian limestone, Deep Sea Drilling Project Site 465, Section 465A-38-3. In Thiede, J., Vallier, T.L., et al., *Init. Repts. DSDP, 62*: Washington (U.S. Govt. Printing Office), 923–937.
- Didyk, B.M., Simoneit, B.R.T., Brassell, S.C., and Eglinton, G., 1978. Organic geochemical indicators of palaeoenvironmental conditions of sedimentation. *Nature*, 272:216–222.
- Espitalié, J., Laporte, J.L., Madec, M., Marquis, F., Leplat, P., Paulet, J., and Boutefeu, A., 1977. Méthode rapide de caractérisation des roches mères, de leur potentiel pétrolier et de leur degré d'évolution. *Rev. Inst. Fr. Pet.*, 32:23–42.
- Farrimond, P., Eglinton, G., Brassell, S.C., and Jenkyns, H.C., 1990. The Cenomanian/Turonian anoxic event in Europe: an organic geochemical study. *Mar. Pet. Geol.*, 7:75–89.
- Fischer, A.G., and Arthur, M.A., 1977. Secular variations in the pelagic realm. In Cook, H.E., and Enos, P. (Eds.), *Deep Water Carbonate Environments*. Spec. Publ.—Soc. Econ. Paleontol. Mineral., 25:19–50.
- Gelpi, E., Schneider, H., Mann, J., and Oró, J., 1970. Hydrocarbons of geochemical significance in microscopic algae. *Phytochemistry*, 9:603–612.
- Goossens, H., de Leeuw, J.W., Schenck, P.A., and Brassell, S.C., 1984. Tocopherols as likely precursors of pristane in ancient sediment and crude oils. *Nature*, 312:440–442.

- Han, J., and Calvin, M., 1969. Hydrocarbon distribution of algae and bacteria, and microbiological activity in sediments. *Proc. Natl. Acad. Sci. U.S.A.*, 64:436–443.
- Huang, W.-Y., and Meinschein, W.G., 1979. Sterols as ecological indicators. *Geochim. Cosmochim. Acta*, 43:739–745.
- Jenkyns, H.C., 1980. Cretaceous anoxic events: from continents to oceans. *J. Geol. Soc. (London, U.K.)*, 137:171–188.
- Kimble, B.J., Maxwell, J.R., Philp, R.P., Eglinton, G., Albrecht, P., Ensminger, A., Arpino, P., and Ourisson, G., 1974. Tri- and tetraterpenoid hydrocarbons in the Messel oil shale. *Geochim. Cosmochim. Acta*, 38:1165–1181.
- Kok, M.D., Schouten, S., and Sinninghe Damsté, J.S., 2000. Formation of insoluble, nonhydrolyzable, sulfur-rich macromolecules via incorporation of inorganic sulfur species into algal carbohydrates. *Geochim. Cosmochim. Acta*, 64:2689–2699.
- Koopmans, M.P., de Leeuw, J.W., Lewan, M.D., and Sinninghe Damsté, J.S., 1996a. Impact of dia- and catagenesis on sulphur and oxygen sequestration of biomarkers as revealed by artificial maturation of an immature sedimentary rock. *Org. Geochem.*, 25:391–426.
- Koopmans, M.P., Köster, J., van Kaam-Peters, H.M.E., Kenig, F., Schouten, S., Hartgers, W.A., de Leeuw, J.W., and Sinninghe Damsté, J.S., 1996b. Dia- and catagenetic products of isorenieratene: molecular indicators of photic zone anoxia. *Geochim. Cosmochim. Acta*, 60:4467–4496.
- Koopmans, M.P., Rijpstra, W.I.C., Klapwijk, M.M., de Leeuw, J.W., Lewan, M.D., and Sinninghe Damsté, J.S., 1999. A thermal and chemical degradation approach to decipher pristane and phytane precursors in sedimentary organic matter. *Org. Geochem.*, 30:1089–1104.
- Köster, J., van Kaam-Peters, H.M.E., Koopmans, M.P., de Leeuw, J.W., and Sinninghe Damsté, J.S., 1997. Sulphurization of homohopanooids: effects on carbon number distribution, speciation, and 22S/22R epimer ratios. *Geochim. Cosmochim. Acta*, 61:2431–2452.
- Kuypers, M.M.M., Pancost, R.D., Nijenhuis, I.A., and Sinninghe Damsté, J.S., 2002. Enhanced productivity led to increased organic carbon burial in the euxinic North Atlantic Basin during the late Cenomanian oceanic anoxic event. *Paleoceanography*, 17:10.1029/2002PA000569.
- Larson, R.L., 1991a. Geological consequences of superplumes. *Geology*, 19:963–966.
- Larson, R.L., 1991b. Latest pulse of Earth: evidence for a mid-Cretaceous super plume. *Geology*, 19:547–550.
- Mackenzie, A.S., Brassell, S.C., Eglinton, G., and Maxwell, J.R., 1982. Chemical fossils: the geological fate of steroids. *Science*, 217:491–504.
- Marlowe, I.T., Brassell, S.C., Eglinton, G., and Green, J.C., 1990. Long-chain alkenones and alkyl alkenoates and the fossil coccolith record of marine sediments. *Chem. Geol.*, 88:349–375.
- Metzger, P., Allard, B., and Casadevall, E., 1990. Structure and chemistry of a new chemical race of *Botryococcus braunii* that produces lycopadiene, a tetraterpenoid hydrocarbon. *J. Phycol.*, 26:258–266.
- Meyers, P.A., Trull, T.W., and Kawaka, O.E., 1984. Organic geochemical comparison of Cretaceous green and black claystones from Hole 530A in the Angola Basin. In Hay, W.W., Sibuet, J.C., et al., *Init. Repts. DSDP*, 75 (Pt. 2): Washington (U.S. Govt. Printing Office), 1009–1018.
- Moldowan, J.M., Seifert, W.K., and Gallegos, E.J., 1985. Relationship between petroleum composition and depositional environment of petroleum source rocks. *AAPG Bull.*, 69:1255–1268.
- Ourisson, G., Albrecht, P., and Rohmer, M., 1979. The hopanooids: paleochemistry and biochemistry of a group of natural products. *Pure Appl. Chem.*, 51:709–729.
- Ourisson, G., and Rohmer, M., 1992. Hopanooids. 2. Biohopanooids: a novel class of bacterial lipids. *Acc. Chem. Res.*, 25:403–408.
- Ourisson, G., Rohmer, M., and Poralla, K., 1987. Prokaryotic hopanooids and other polyterpenoid sterol surrogates. *Annu. Rev. Microbiol.*, 41:301–333.

- Peters, K.E., 1986. Guidelines for evaluating petroleum source rock using programmed pyrolysis. *AAPG Bull.*, 70:318–329.
- Peters, K.E., and Moldowan, J.M., 1991. Effects of source, thermal maturity, and biodegradation on the distributions and isomerization of homohopanes in petroleum. *Org. Geochem.*, 17:47–61.
- Peters, K.E., and Moldowan, J.M., 1993. *The Biomarker Guide: Interpreting Molecular Fossils in Petroleum and Ancient Sediments*: Englewood Cliffs, NJ (Prentice Hall).
- Ryan, W.B.F., and Cita, M.B., 1977. Ignorance concerning episodes of ocean-wide stagnation. *Mar. Geol.*, 23:197–215.
- Schlanger, S.O., and Jenkyns, H.C., 1976. Cretaceous oceanic anoxic events: causes and consequences. *Geol. Mijnbouw*, 55:179–184.
- Seifert, W.K., and Moldowan, J.M., 1980. The effect of thermal stress on source-rock quality as measured by hopane stereochemistry. *Phys. Chem. Earth*, 12:229–237.
- Silliman, J.E., Meyers, P.A., Ostrom, P.H., Ostrom, N.E., and Eadie, B.J., 2000. Insights to the origin of perylene from isotopic analyses of sediments from Saanich Inlet, British Columbia. *Org. Geochem.*, 31:1133–1142.
- Sinninghe Damsté, J.S., Kuypers, M.M.M., Schouten, S., Schulte, S., and Rullkötter, J., 2003. The lycopane/C₃₁ *n*-alkane ratio as a proxy to assess palaeoxicity during sediment deposition. *Earth Planet. Sci. Lett.*, 209:215–226.
- Sinninghe Damsté, J.S., Rijpstra, W.I.C., and Reichart, G.-J., 2002. The influence of oxic degradation on the sedimentary biomarker record II. Evidence from Arabian Sea sediments. *Geochim. Cosmochim. Acta*, 66:2737–2754.
- Sinninghe Damsté, J.S., Wakeham, S.G., Kohonen, M.E.L., Hayes, J.M., and de Leeuw, J.W., 1993. A 6,000-year sedimentary molecular record of chemocline excursions in the Black Sea. *Nature*, 362:827–829.
- Stein, R., 1986. Surface-water paleo-productivity as inferred from sediments deposited in oxic and anoxic deep-water environments of the Mesozoic Atlantic Ocean. In Degens, E.T., Meyers, P.A., and Brassel, S.C. (Eds.), *Biogeochemistry of Black Shales*. Mitt. Geol.-Palaeontol. Inst. Univ. Hamburg, 60:55–70.
- Summons, R.E., Jahnke, L.L., Hope, J.M., and Logan, G.A., 1999. 2-Methylhopanoids as biomarkers for cyanobacterial oxygenic photosynthesis. *Nature*, 400:554–557.
- Valisollalao, J., Perakis, N., Chappe, B., and Albrecht, P., 1984. A novel sulphur-containing C₃₅ hopanoid in sediments. *Tetrahedron Lett.*, 25:1183–1186.
- Volkman, J.K., 1986. A review of sterol markers for marine and terrigenous organic matter. *Org. Geochem.*, 9:83–99.
- Volkman, J.K., 1988. Biological marker compounds as indicators of the depositional environments of petroleum source rocks. In Fleet, A.J., Kelts, K., and Talbot, M.R. (Eds.), *Lacustrine Petroleum Source Rocks*. Geol. Soc. Spec. Publ., 40:103–122.
- Volkman, J.K., 1998. Microalgal biomarkers: a review of recent research developments. *Org. Geochem.*, 29:1163–1179.
- Volkman, J.K., and Maxwell, J.R., 1986. Acyclic isoprenoids as biological markers. In Johns, R.B. (Ed.), *Biological Markers in the Sedimentary Record*: New York (Elsevier), 1–42.
- Wakeham, S.G., Freeman, K.H., Pease, T.K., and Hayes, J.M., 1993. A photoautotrophic source for lycopane in marine sediments. *Geochim. Cosmochim. Acta*, 57:159–166.
- Wakeham, S.G., Schaffner, C., Giger, W., Boon, J.J., and de Leeuw, J.W., 1979. Perylene in sediments from the Namibian shelf. *Geochim. Cosmochim. Acta*, 43:1141–1144.
- Werne, J.P., Hollander, D.J., Behrens, A., Schaeffer, P., Albrecht, P., and Sinninghe Damsté, J.S., 2000. Timing of early diagenetic sulfurization of organic matter: a precursor-product relationship in Holocene sediments of the anoxic Cariaco Basin, Venezuela. *Geochim. Cosmochim. Acta*, 64:1741–1751.

Figure F1. Chromatograms showing *n*-alkanes and isoprenoids of two representative samples. Numbers by the peaks give the number of carbon atoms in *n*-alkanes (Pr = pristane, Ph = phytane). **A.** Ion chromatogram *m/z* 57 of Sample 207-1258B-55R-1, 49–50 cm. This distribution pattern is typical for a predominantly algal marine signal and represents the most common sample type. **B.** Ion chromatogram *m/z* 57 of Sample 207-1257B-22R-1, 44–45 cm. This sample is dominated by high amounts of terrigenous input.

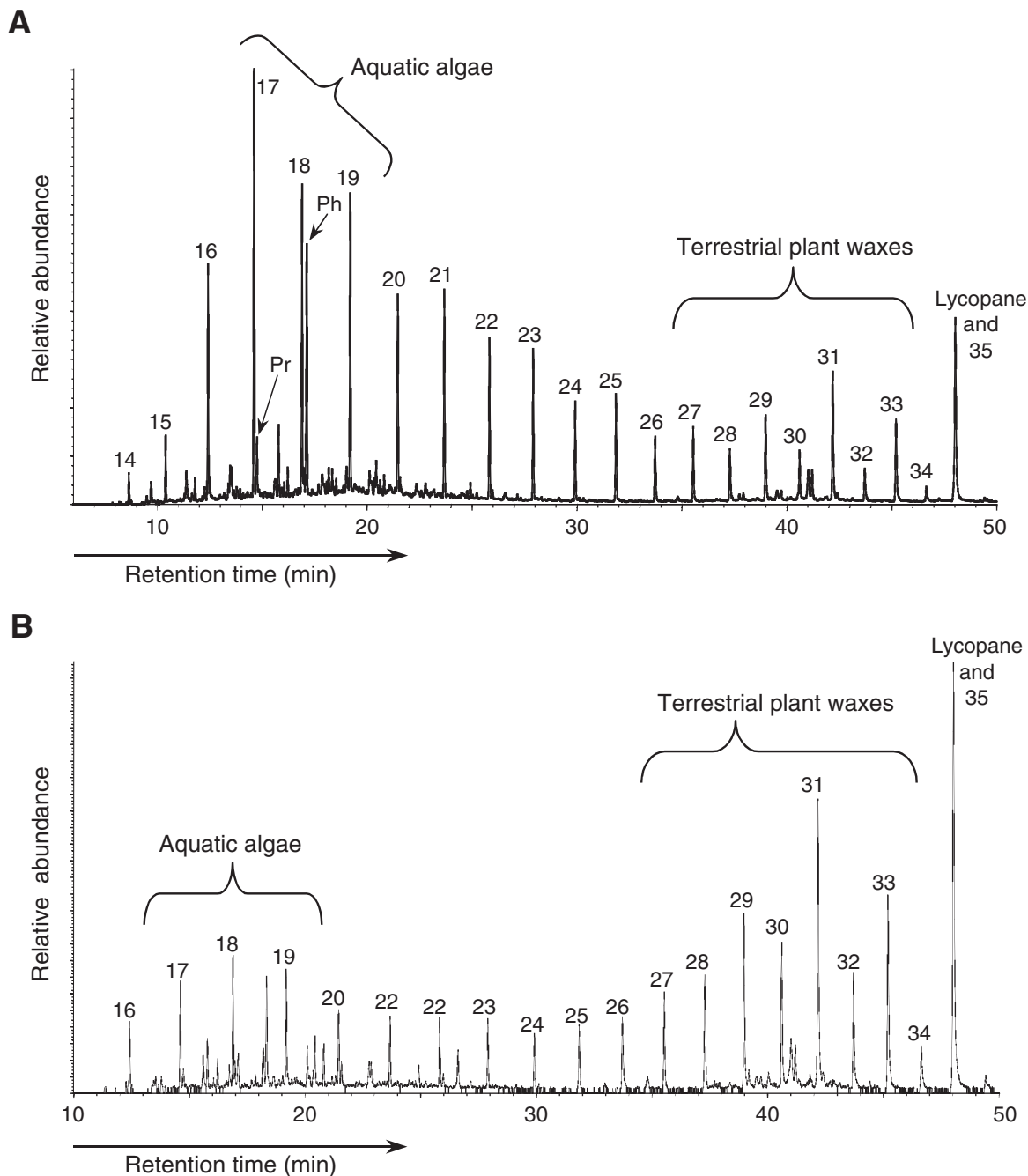


Figure F2. Biomarkers in the partial total ion chromatogram of Sample 207-1258B 55R-1, 49–50 cm. Table T4, p. 22, lists identifications of compounds indicated by small numbers. Colors are used to highlight various groups of biomarkers. Blue = *n*-alkanes, yellow = steranes, orange = sterenes, green = hopanoids, multicolored peaks = coelution of two or more compounds.

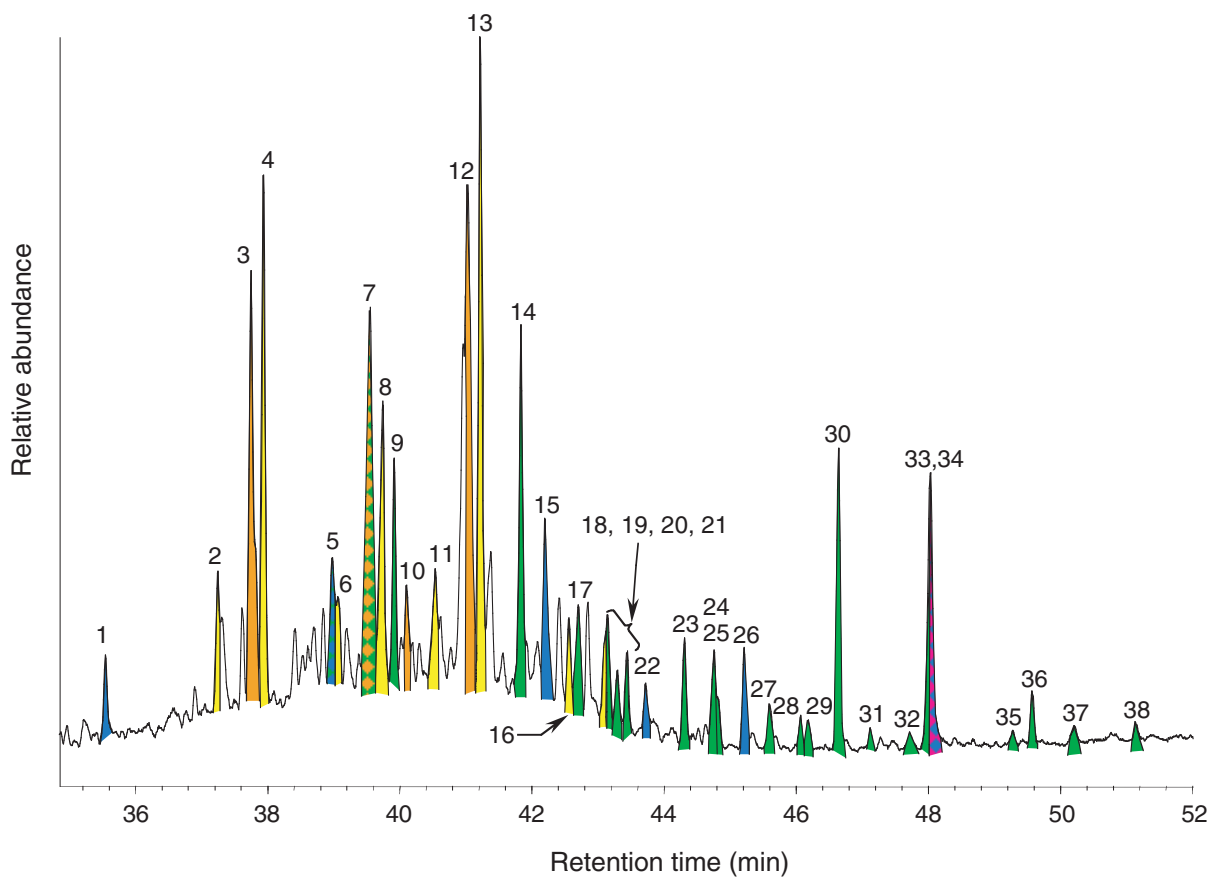


Table T1. Stratigraphic and bulk organic matter properties of Leg 207 samples extracted for biomarker contents.

| Hole, core, section, interval (cm) | Depth | | Age | CaCO ₃ (wt%) | TOC (wt%) | C/N (atomic) | T _{rmax} (°C) | HI (mg HC/g) | OI (mg CO ₂ /g) | Sample (g) | Extract (mg) | Extract (mg/g TOC) | Extract color | Fluorescence |
|---------------------------------------|--------|--------|------------|----------------------------|--------------|-----------------|---------------------------|-----------------|-------------------------------|---------------|-----------------|-----------------------|-----------------------|--------------|
| | (mbsf) | (mcd) | | | | | | | | | | | | |
| 207- | | | | | | | | | | | | | | |
| 1257B-20R-1, 77–78 | 189.47 | 195.60 | Coniacian | 49.8 | 9.65 | 33.0 | 385 | 686 | 34 | 1.0 | 2.6 | 27.0 | Reddish brown | None |
| 1257B-22R-1, 44–45 | 198.74 | 204.87 | Turonian | 7.7 | 9.72 | 30.1 | 402 | 622 | 18 | 1.0 | 0.8 | 8.2 | Reddish brown | None |
| 1257B-24R-4, 32–33 | 212.28 | 218.41 | Turonian | 41.3 | 8.62 | 32.7 | 402 | 679 | 26 | 1.0 | 6.0 | 69.4 | Reddish brown | None |
| 1257C-15R-1, 70–71 | 217.30 | 219.85 | Cenomanian | 56.2 | 8.21 | 32.3 | 397 | 685 | 40 | 1.0 | 2.0 | 23.9 | Reddish brown | None |
| 1258B-44R-4, 75–76 | 397.46 | 417.90 | Turonian | 55.1 | 8.78 | 31.0 | ND | ND | ND | 3.2 | 3.5 | 12.3 | Light reddish brown | None |
| 1258A-43R-2, 64–65 | 401.32 | 426.20 | Turonian | 46.9 | 11.89 | 30.7 | 401 | 577 | 26 | 3.6 | 14.9 | 34.8 | Dark green | None |
| 1258B-46R-2, 56–57 | 404.30 | 426.36 | Cenomanian | 23.4 | 28.13 | 37.0 | 398 | 485 | 24 | 3.1 | 61.0 | 69.8 | Very dark green/brown | None |
| 1258B-51R-2, 40–41 | 428.12 | 452.44 | Cenomanian | 49.4 | 11.63 | 32.9 | ND | ND | ND | 3.0 | 14.9 | 42.3 | Red/orange | Slight |
| 1258B-55R-1, 49–50 | 445.99 | 470.31 | Cenomanian | 43.7 | 8.80 | 32.6 | 402 | 610 | 27 | 3.2 | 5.7 | 20.0 | Red/orange | Slight |
| 1258C-31R-2, 26–27 | 468.16 | 500.66 | Albian | 12.5 | 4.54 | 26.9 | 415 | 499 | 64 | 6.6 | 8.1 | 27.0 | Clear–yellow | Vivid |

Notes: HI = hydrogen index, OI = oxygen index. TOC = total organic carbon. ND = not determined.

Table T2. Biomarker-based parameters for organic matter thermal maturity and degree of preservation.

| Hole, core, section | Depth (mcd) | Age | TOC (wt%) | Maturity parameters | | | Preservation parameters | | | | |
|---------------------|-------------|------------|-----------|---|---|--|-------------------------|-------------------------------------|---|------------------------|---|
| | | | | $C_{31}\text{-}\beta\beta/(\alpha\beta+\beta\alpha+\beta\beta)$ | $C_{30}\text{-}\beta\beta\text{-}R/(\alpha\beta\text{-}S+\alpha\beta\text{-}R)$ | $C_{31}\text{-}\alpha\beta\text{-}R/(\alpha\beta\text{-}S+\alpha\beta\text{-}R)$ | homohopane index | thiophenes/ $C_{30}\text{-}hopanes$ | $(\text{lycopane} + n\text{-}C_{35})/n\text{-}C_{31}$ | isorenieratane-thianes | |
| 207- | | | | | | | | | | | |
| 1257B-20R-1 | 195.60 | Coniacian | 9.65 | NA | 0.9 | 0.8 | 7.0 | 0.02 | 2.2 | | + |
| 1257B-22R-1 | 204.87 | Turonian | 9.72 | 0.9 | 0.8 | NA | 6.2 | 0.2 | 1.8 | | - |
| 1257B-24R-4 | 218.41 | Turonian | 8.62 | 0.8 | 0.9 | 0.7 | 6.5 | 0.2 | 4.9 | | - |
| 1257C-15R-1 | 219.85 | Cenomanian | 8.21 | NA | 0.9 | NA | 7.1 | 0.3 | 4.4 | | - |
| 1258B-44R-4 | 417.90 | Turonian | 8.78 | 0.8 | 0.9 | 0.8 | 9.6 | 0.3 | 16.0 | | + |
| 1258A-43R-2 | 426.20 | Turonian | 11.89 | 0.7 | 0.9 | 0.8 | 8.5 | 0.3 | 11.1 | | - |
| 1258B-46R-2 | 426.36 | Cenomanian | 28.13 | 0.7 | 0.8 | 0.9 | 10.1 | 0.05 | 2.2 | | + |
| 1258B-51R-2 | 452.44 | Cenomanian | 11.63 | 0.6 | 0.8 | 0.7 | 10.6 | 0.3 | 2.4 | | + |
| 1258B-55R-1 | 470.31 | Cenomanian | 8.80 | 0.6 | 0.9 | 0.9 | 10.5 | 0.3 | 1.9 | | + |
| 1258C-31R-2 | 500.66 | Albian | 4.54 | 0.7 | 0.8 | 0.7 | 7.4 | 0.3 | 0.8 | | - |

Notes: Homohopane index = percentage of $\beta\beta$ -pentakishomohopane in $\Sigma C_{31}\text{-}C_{35}$ $\beta\beta$ -homohopanes (modified from Peters and Moldowan, 1991). NA = not applicable. +/- = presence/absence of isorenieratane thianes.

Table T3. Source-indicative biomarker ratios and distributions in organic matter in Leg 207 samples.

| Hole, core, section | Depth (mcd) | Age | TOC (wt%) | <i>m/z</i> 57 | | | | | | $\alpha\alpha$ -R steranes (<i>m/z</i> 217) | | | | | <i>m/z</i> 217/191 |
|---------------------|-------------|------------|-----------|---------------------------------|-------------------------------|-------------------------------------|---|-----|-------|--|----------------------------|----------------------------|---|---|--------------------|
| | | | | <i>C</i> _{max} aquatic | <i>C</i> _{max} waxes | MAC | <i>n</i> -C ₁₇ / <i>n</i> -C ₃₁ | CPI | Pr/Ph | <i>C</i> ₂₇ (%) | <i>C</i> ₂₈ (%) | <i>C</i> ₂₉ (%) | <i>C</i> ₂₇ / <i>C</i> ₂₉ | <i>C</i> ₂₈ / <i>C</i> ₂₇ | Steranes/hopanes |
| 207- | | | | | | | | | | | | | | | |
| 1257B-20R-1 | 195.60 | Coniacian | 9.65 | <i>n</i> -C ₁₈ | <i>n</i> -C ₃₁ | <i>n</i> -C ₁₈ | 1.3 | 1.7 | 0.9 | 34 | 26 | 41 | 0.83 | 0.76 | 0.4 |
| 1257B-22R-1 | 204.87 | Turonian | 9.72 | <i>n</i> -C ₁₈ | <i>n</i> -C ₃₁ | Lycopane/ <i>n</i> -C ₃₅ | 0.2 | 1.5 | 0.8 | 29 | 24 | 46 | 0.64 | 0.82 | 0.3 |
| 1257B-24R-4 | 218.41 | Turonian | 8.62 | <i>n</i> -C ₁₆ | <i>n</i> -C ₃₁ | <i>n</i> -C ₁₆ | 2.2 | 1.8 | 1.8 | 34 | 23 | 43 | 0.78 | 0.69 | 0.7 |
| 1257C-15R-1 | 219.85 | Cenomanian | 8.21 | <i>n</i> -C ₁₇ | <i>n</i> -C ₃₁ | Lycopane/ <i>n</i> -C ₃₅ | 1.1 | 2.1 | 0.3 | 38 | 24 | 38 | 0.99 | 0.64 | 0.8 |
| 1258B-44R-4 | 417.90 | Turonian | 8.78 | <i>n</i> -C ₁₆ | <i>n</i> -C ₃₁ | <i>n</i> -C ₁₆ | 6.0 | 1.3 | 0.6 | 35 | 29 | 36 | 0.97 | 0.85 | 0.3 |
| 1258A-43R-2 | 426.20 | Turonian | 11.89 | <i>n</i> -C ₁₈ | <i>n</i> -C ₃₃ | Lycopane/ <i>n</i> -C ₃₅ | 1.0 | 2.0 | 0.3 | 35 | 27 | 38 | 0.91 | 0.76 | 0.2 |
| 1258B-46R-2 | 426.36 | Cenomanian | 28.13 | Phytane | <i>n</i> -C ₂₇ | Phytane | 1.3 | 2.7 | 0.3 | 30 | 23 | 47 | 0.64 | 0.78 | 0.3 |
| 1258B-51R-2 | 452.44 | Cenomanian | 11.63 | <i>n</i> -C ₁₇ | <i>n</i> -C ₃₁ | <i>n</i> -C ₁₇ | 4.2 | 1.4 | 0.3 | 36 | 22 | 42 | 0.87 | 0.62 | 0.5 |
| 1258B-55R-1 | 470.31 | Cenomanian | 8.80 | <i>n</i> -C ₁₇ | <i>n</i> -C ₃₁ | <i>n</i> -C ₁₇ | 2.4 | 1.8 | 0.4 | 37 | 24 | 39 | 0.95 | 0.64 | 0.5 |
| 1258C-31R-2 | 500.66 | Albian | 4.54 | Phytane | <i>n</i> -C ₂₉ | Phytane | 0.4 | 3.2 | 0.3 | 41 | 19 | 40 | 1.01 | 0.47 | 0.2 |

Notes: *C*_{max} aquatic [waxes] = dominant *n*-alkane between *n*-C₁₆ and *n*-C₁₈ [*n*-C₂₃ and *n*-C₃₃]. MAC = most abundant compound. CPI = carbon preference index (Bray and Evans, 1961). Pr/Ph = pristane/phytane. *m/z* = atomic mass/charge ratio.

Table T4. Identifications of biomarker compounds in TIC.

| Peak number | Compound identification |
|-------------|--|
| 1 | <i>n</i> -C ₂₇ alkane |
| 2 | 5β,14α,17α(H)-20R-cholestane |
| 3 | cholest-4-ene |
| 4 | 5α,14α,17α(H)-20R-cholestane and cholest-5-ene |
| 5 | C ₂₇ 17α(H)-trisnorhopane (Tm) and <i>n</i> -C ₂₉ alkane |
| 6 | 20R-5β,14α,17α(H)-24-methylcholestane |
| 7 | C ₂₇ 17β(H)-trisnorhopane (Tm) and 24-methylcholest-4-ene |
| 8 | 20R-5α,14α,17α(H)-24-methylcholestane and 24-methylcholest-5-ene |
| 9 | 30-norneohop-13(18)-ene |
| 10 | 24-ethyl-cholestadiene |
| 11 | 20R-5β,14α,17α(H)-24-ethylcholestane |
| 12 | 24-ethylcholest-4-ene |
| 13 | 20R-5α,14α,17α(H)-24-ethylcholestane and 24-ethylcholest-5-ene |
| 14 | hop-17(21)-ene |
| 15 | <i>n</i> -C ₃₁ alkane |
| 16 | methyl-C ₃₀ -sterane and methyl-C ₃₀ -sterene |
| 17 | 17α,21β(H)-hopane |
| 18 | 17β,21β(H)-30-norhopane |
| 19 | Unidentified hopene |
| 20 | C ₃₁ -22S-homohop-17(21)-ene |
| 21 | C ₃₁ -22R-homohop-17(21)-ene |
| 22 | <i>n</i> -C ₃₂ alkane |
| 23 | C ₃₁ -17α,21β(H)-22R-homohopane |
| 24 | C ₃₀ -17β,21β(H)-hopane |
| 25 | C ₃₁ -17β,21α(H)-homohopane |
| 26 | <i>n</i> -C ₃₃ alkane |
| 27 | C ₃₂ -17α,21β(H)-homohopane |
| 28 | Unidentified hopene |
| 29 | C ₃₂ -17β,21α(H)-homohopane |
| 30 | C ₃₁ -17β,21β(H)-homohopane |
| 31 | C ₃₃ -17α,21β(H)-homohopane |
| 32 | C ₃₃ -17β,21α(H)-homohopane |
| 33 | C ₃₂ -17β,21β(H)-homohopane |
| 34 | Lycopane and <i>n</i> -C ₃₅ alkane |
| 35 | C ₃₅ -homohop-17(21)-ene |
| 36 | C ₃₃ -17β,21β(H)-homohopane |
| 37 | C ₃₅ -17α,21β(H)-homohopane |
| 38 | C ₃₄ -17β,21β(H)-homohopane |

Note: TIC from Sample 207-1258B-55R-1, 49–50 cm, shown in Figure F2, p. 18.